

Surface gravity waves in deep fluid at vertical shear flows

G. Gogoberidze,* L. Samushia, G. D. Chagelishvili, and J. G. Lominadze

*Center for Plasma Astrophysics,
Abastumani Astrophysical Observatory,
Ave. A. Kazbegi 2a, Tbilisi 0160, Georgia*

W. Horton

Institute for Fusion Studies, The University of Texas at Austin, Austin, Texas 78712

(Dated: October 30, 2018)

Abstract

Special features of surface gravity waves in deep fluid flow with constant vertical shear of velocity is studied. It is found that the mean flow velocity shear leads to non-trivial modification of surface gravity wave modes dispersive characteristics. Moreover, the shear induces generation of surface gravity waves by internal vortex mode perturbations. The performed analytical and numerical study provides, that surface gravity waves are effectively generated by the internal perturbations at high shear rates. The generation is different for the waves propagating in the different directions. Generation of surface gravity waves propagating along the main flow considerably exceeds the generation of surface gravity waves in the opposite direction for relatively small shear rates, whereas the later wave is generated more effectively for the high shear rates. From the mathematical point of view the wave generation is caused by non self-adjointness of the linear operators that describe the shear flow.

PACS numbers: 92.10.Hm, 47.35.+i, 47.27.Pa

*Electronic address: gogober@geo.net.ge

I. INTRODUCTION

Generation of surface gravity waves (SGW), that are the best known sea and oceanic waves, are naturally associated with winds. Momentum transfer from wind to undulating movement of the ocean which is the basic mechanism of surface waves generation, is investigated since Kelvin's pioneering work [1]. Independent and inter-complementary theories of Phillips [2] and Miles [3, 4, 5, 6] provide the basics of theoretical understanding of surface wave generation by wind. Phillips' resonant mechanism is responsible for excitation and initial rising of wave motion on unexcited surface of the fluid; Miles' mechanism — energy transfer from wind to fluid as a consequence of wind shear flow and surface waves interaction — is responsible for subsequent amplification of the waves. According to Miles' mechanism the energy source is wind shear flows situated outside the fluid. Other ways of SGW generation have been also studied such as the possibility of SGW generation by earthquakes [7, 8] and theory of SGW generation by intra-fluid explosions [9]. In theories mentioned above sources of SGW generation are extrinsic for the fluid.

The question arises as to whether intrinsic for the fluid sources (shear flows and vortex perturbations for example) could generate SGW.

This question become especially interesting in view of the impressive progress made in the understanding of spectrally stable shear flow phenomena by hydrodynamic community in the past ten years. The early transient period for the perturbations has been shown to reveal rich and complicate behavior in smooth (without inflection point) shear flows. Particularly, it has been shown that the linear dynamics of perturbations in the flows are accompanied by intense temporal energy exchange processes between background flow and perturbations and/or between different modes of perturbations. From the mathematical point of view these effects are caused by the non-self adjointness of the linear operators in shear flows and are adequately described in the framework of so-called non-modal approach (see, e.g., [10, 11, 12]). The non-modal approach implies a change of independent variables from the laboratory frame to a moving frame and the study of temporal evolution of *spatial Fourier harmonics* (SFHs) of perturbations without any spectral expansion in time.

We examine the linear dynamics of surface waves and internal perturbations in deep fluid in the absence of wind and presence of the fluid flow with vertical shear of velocity. Dispersive characteristics of shear modified SGWs as well as linear mechanism of surface waves generation in deep fluid by internal perturbations is studied in detail in the framework of the non-modal approach.

The paper is organized as follows: mathematical formalism is presented in Sec. II. Shear modified SGWs and their generation is analyzed in Sec. III. Applications of the obtained results to the concrete physical problems are discussed in Sec. IV. Conclusions are given in Sec. V.

II. MATHEMATICAL FORMALISM

Consider deep fluid with flat outer surface at $z = 0$ and constant shear flow $\mathbf{U}_0 = (Az, 0, 0)$ for $z < 0$. The shear parameter A is considered to be positive for the simplicity. The gravitational field is considered to be uniform $\mathbf{g} = (0, 0, -g)$. Generally, four modes of perturbation: SGW, internal gravity waves, sound waves and vortex mode can exist in the system. To reduce the mathematical complications as much as possible but still keep the basic physics of our analysis, we consider fluid to be incompressible (which drops sound waves) and neglect the stratification effects (assuming that frequency of internal gravity waves is much less in comparison with the frequency of SGWs, i.e., considering internal gravity waves as aperiodic/vortex mode perturbations). In further analysis we ignore also effects of viscosity. After these simplifications we maintain just two modes of perturbation - SGW and vortex mode and write up the following differential equations for the linear dynamics of perturbations of velocity (\mathbf{u}') and normalized pressure ($p' = p/\rho_0$):

$$\frac{\partial u'_x}{\partial x} + \frac{\partial u'_y}{\partial y} + \frac{\partial u'_z}{\partial z} = 0, \quad (1)$$

$$\frac{\partial u'_x}{\partial t} + Az \frac{\partial u'_x}{\partial x} + Au'_z = -\frac{\partial p'}{\partial x}, \quad (2)$$

$$\frac{\partial u'_y}{\partial t} + Az \frac{\partial u'_y}{\partial x} = -\frac{\partial p'}{\partial y}, \quad (3)$$

$$\frac{\partial u'_z}{\partial t} + Az \frac{\partial u'_z}{\partial x} = -\frac{\partial p'}{\partial z}, \quad (4)$$

with the boundary condition on the surface $z = 0$:

$$\left(\frac{\partial p'}{\partial t} - gu'_z \right) \Big|_{z=0} = 0. \quad (5)$$

Further we use the standard technique of the non-modal approach [10]: introduction of co-moving variables ($x' = x + Azt, y' = y, z' = z, t' = t$) let us to transform spatial inhomogeneity presented in Eqs. (1)-(5) to temporal one. Then, after the Fourier transform with respect to x' and y' :

$$\mathbf{u}'(\mathbf{r}, t) = \frac{1}{4\pi^2} \int \mathbf{u}(k_x, k_y, z', t) \exp[i(k_x x' + k_y y')] dk_x dk_y, \quad (6)$$

the dynamic equations are reduced to:

$$ik_x u_x + ik_y u_y + \left(\frac{\partial}{\partial z'} - iAt'k_x \right) u_z = 0, \quad (7)$$

$$\frac{\partial u_x}{\partial t'} + Au_z = -ik_x p, \quad (8)$$

$$\frac{\partial u_y}{\partial t'} = -ik_y p, \quad (9)$$

$$\frac{\partial u_z}{\partial t'} = - \left(\frac{\partial}{\partial z'} - iAt'k_x \right) p, \quad (10)$$

$$\left(\frac{\partial p}{\partial t'} - gu_z \right) \Big|_{z'=0} = 0. \quad (11)$$

Hereafter primes of z' and t' variables will be omitted.

From this set we readily obtain the following equation for the perturbation of vertical component of velocity:

$$\frac{\partial}{\partial t} \left(\left[\tilde{k}^2 - \left(\frac{\partial}{\partial z} - iAtk_x \right)^2 \right] u_z \right) = 0, \quad (12)$$

where $\tilde{k} = \sqrt{k_x^2 + k_y^2}$.

All other perturbed quantities (u_x , u_y and p) can be readily expressed through u_z combining Eqs. (7)-(10); e.g., for p we have:

$$p = -\frac{1}{\tilde{k}^2} \left(\frac{\partial}{\partial t} \left[\left(\frac{\partial}{\partial z} - iAtk_x \right) u_z \right] - iAk_x u_z \right), \quad (13)$$

Integration of Eq. (12) with respect to time yields:

$$\left[\tilde{k}^2 - \left(\frac{\partial}{\partial z} - iAtk_x \right)^2 \right] u_z(k_x, k_y, z, t) = F(k_x, k_y, z), \quad (14)$$

where $F(k_x, k_y, z)$ is the constant (in time) of integration and defines the internal vortex mode perturbation in the flow: $F(k_x, k_y, z) = 0$ relates to a case when the internal perturbation is absent.

Fourier transformation with respect to z :

$$\begin{bmatrix} u_z(k_x, k_y, z, t) \\ F(k_x, k_y, z) \end{bmatrix} = \frac{1}{2\pi} \int_{-\infty}^{\infty} \begin{bmatrix} u_z(k_x, k_y, k_z, t) \\ \tilde{F}(k_x, k_y, k_z) \end{bmatrix} e^{ik_z z} dk_z \quad (15)$$

reduces Eq. (14) to the following one:

$$k^2(t)u_z(k_x, k_y, k_z, t) = \tilde{F}(k_x, k_y, k_z) + 4i\pi\tilde{k}C(k_x, k_y, t), \quad (16)$$

where

$$C \equiv \frac{1}{4i\pi\tilde{k}} \left[\left(\frac{d}{dz} - 2iAtk_x - ik_z \right) u_z(k_x, k_y, z, t) \right] \Big|_{z=0}. \quad (17)$$

Defining $u_z(k_x, k_y, k_z, t)$ from Eq. (16), making invert Fourier transform with respect to k_z , taking into account boundary condition $|u_z| < \infty$ at $z = -\infty$ and the fact that $C(k_z, k_y, t)$ does not depend on z , we obtain:

$$\begin{aligned} u_z(k_x, k_y, z, t) &= \frac{1}{2\pi} \int_{-\infty}^{\infty} \frac{\tilde{F}(k_x, k_y, k_z)}{k^2(t)} \exp(ik_z z) dk_z + \\ &+ C(k_x, k_y, t) \exp[(\tilde{k} + iAtk_x)z], \end{aligned} \quad (18)$$

where $k^2(t) = \tilde{k}^2 + k_z^2(t)$; $k_z(t) \equiv k_z - Atk_x$.

The first term in Eq. (18) relates to the vortex mode perturbation [11, 13], whereas the second term, which is exponentially decreasing with the depth, relates to the SFHs of shear modified surface waves.

Substituting Eq. (18) into Eq. (13), and using boundary condition, Eq. (11), we obtain:

$$\frac{d^2 C}{dt^2} + \frac{iAk_x}{\tilde{k}} \frac{dC}{dt} + \tilde{k}gC = I(k_x, k_y, t), \quad (19)$$

where

$$I(k_x, k_y, t) \equiv \int_{-\infty}^{\infty} \left[8iA^2 k_x^2 \tilde{k} \frac{k_z(t)}{k^6(t)} - \frac{\tilde{k}g}{k^2(t)} \right] \tilde{F}(\mathbf{k}) dk_z. \quad (20)$$

Generally, Eqs. (19)-(20) describe the dynamics of surface wave SFHs in the presence of the internal vortical source - the term $I(k_x, k_y, t)$ is the result of an interplay of the mean flow shear and the internal vortical perturbations and couples the later perturbation with the surface one. So, there is no coupling between these perturbations in the absence of the shear. Indeed, if there are no surface perturbations initially [$u_z(k_x, k_y, z = 0, t = 0) = 0$], then from Eqs. (16) and (20), one readily obtains that $I(k_x, k_y, t) \sim u_z(k_x, k_y, z = 0, t = 0)$ at $A = 0$, i.e., $I(k_x, k_y, t) \equiv 0$. Thus, if there is no the source in shearless flow initially, it does not appear afterward.

III. SGWS AND THEIR GENERATION IN SHEAR FLOW

One can see from Eqs. (19) and (20), that there are two main effects of the shear: firstly, the second term on the left hand side of Eq. (19) indicates that the velocity shear affects the frequencies of SGWs. Secondly, the source term $I(k_x, k_y, t)$ caused by the internal perturbations, couples the internal and surface perturbations and results the emergence/generation of SGW in the flow. Our further attempts are focused on the study of these effects.

A. Shear modified SGWs

In this subsection we study shear induced modifications of properties of SGWs. For this purposes we assume that initially there were no vortex mode perturbations: $\tilde{F}(k_x, k_y, k_z) = 0$. Consequently, $I(k_x, k_y, t) = 0$ [see Eqs. (20)], and Eq. (19) reduces to the homogeneous one, with the solution:

$$C_h(k_x, k_y, t) = C_1(k_x, k_y) \exp(-i\Omega_1 t) + C_2(k_x, k_y) \exp(-i\Omega_2 t), \quad (21)$$

where $C_{1,2}(k_x, k_y)$ are determined by initial conditions and

$$\Omega_{1,2} = \pm \sqrt{\tilde{k}g + \frac{A^2 k_x^2}{4\tilde{k}^2}} - \frac{Ak_x}{2\tilde{k}} = \sqrt{\tilde{k}g} \left(\pm \sqrt{1 + S^2 \frac{k_x^2}{\tilde{k}^2}} - S \frac{k_x}{\tilde{k}} \right) \quad (22)$$

represents shear modified frequencies of SFH of SGW propagating in opposite directions and $S \equiv A/(4\tilde{k}g)^{1/2}$ is the dimensionless shear rate. This equation provides, that in contrast with acoustic and magnetohydrodynamic wave modes [14, 15, 16], the presence of the shear does not lead to the time variability of the frequency. However, velocity shear leads to the non-trivial modification of the frequencies and consequently phase velocities of SFH [17, 18]. Indeed, for the value of the phase velocity, Eq. (22) provides:

$$V_{ph}(S, \phi) = \sqrt{\frac{g}{k}} \left(\sqrt{1 + S^2 \cos^2 \phi} - S \cos \phi \right), \quad (23)$$

where $\phi \equiv \arccos(k_x/\tilde{k})$.

The phase velocity is isotropic in the shearless limit ($S = 0$), while depends on ϕ in the shear flow. The anisotropy increases with the shear rate. The value of the phase velocity is minimal at $\phi = 0$: $V_{ph}^{\min} = \sqrt{g/\tilde{k}}(\sqrt{1 + S^2} - S)$ and is maximal at $\phi = \pi$: $V_{ph}^{\max} = \sqrt{g/\tilde{k}}(\sqrt{1 + S^2} + S)$. Suppose SGW is emitted by point source situated on the surface at $x = y = 0$. From Eq. (23) it follows that the propagation of the leading wave crest is described by:

$$\begin{aligned} r(S, \phi, t) &= V_{ph}(S, \phi)t = \\ &= \sqrt{\frac{g}{k}} \left(\sqrt{1 + S^2 \cos^2 \phi} - S \cos \phi \right) t. \end{aligned} \quad (24)$$

Figure 1 shows the leading wave crest of the SGW for three different moments of time t_1, t_2, t_3 , when $t_2 = 2t_1, t_3 = 3t_1$, that are circular but not concentric.

B. Generation of SGWs by internal vortices

Let us initially analyze the source term $I(k_x, k_y, t)$ that is determined by $\tilde{F}(k_x, k_y, k_z)$. Assume $\tilde{F}(k_x, k_y, k_z)$ is a localized function in the wavenumber space, with a center of localization at $\mathbf{k}_0 = (k_{x0}, k_{y0}, k_{z0})$. Note that the first multiplier in the integrand of Eq. (20) reaches its maximum when $k_z - Ak_x t = 0$. Consequently, the maximum of the integral is in the vicinity of time $t = t_* \equiv k_{z0}/(Ak_{x0})$. Equation (20) provides, that generally $I(k_x, k_y, t)$ tends to zero in both limits $t \rightarrow \pm\infty$. Actually, it exists some time interval $2\Delta t$ around t_* where the source term differs

from zero. The value of Δt depends on the degree of localization of internal perturbation, i.e., of $\tilde{F}(k_x, k_y, k_z)$ in wavenumber space. (The source localization is demonstrated below on a specific example.) Thus, in the case of a localized source, the coupling between surface (gravity wave) and internal (vortex mode) perturbations takes place in some time interval $2\Delta t$ around t_* , and at $|t - t_*| > \Delta t$ these perturbations can be considered separately.

The general solution of the inhomogeneous equation, Eq. (19), is the sum of the general solution of corresponding homogeneous equation and a particular solution of the equation:

$$C(k_x, k_y, t) = C_h(k_x, k_y, t) + C_i(k_x, k_y, t). \quad (25)$$

The general solution $C_h(k_x, k_y, t)$ is presented by Eq. (21), whereas a particular solution of Eq. (19) is:

$$C_i = \frac{1}{2\Omega_0} \exp(-i\Omega_1 t) \int_{t_0}^t I(k_x, k_y, t') \exp(i\Omega_1 t') dt' - \frac{1}{2\Omega_0} \exp(-i\Omega_2 t) \int_{t_0}^t I(k_x, k_y, t') \exp(i\Omega_2 t') dt', \quad (26)$$

where

$$\Omega_0 = \sqrt{\tilde{k}g + \frac{A^2 k_x^2}{4\tilde{k}^2}} = \sqrt{\tilde{k}g} \sqrt{1 + S^2 \frac{k_x^2}{\tilde{k}^2}}. \quad (27)$$

Assume that the coupling between the surface and internal modes can be neglected at the initial moment of time t_0 , i.e., $t_0 < t_* - \Delta t$. After passing through the coupling time interval, for any $t > t_f = t_* + \Delta t$ the modes become independent again. However, during the time interval $[t_0, t_f]$, internal vortices generate SGWs with frequencies Ω_1 and Ω_2 [see Eq. (22)]. As it follows from Eqs. (21), (25), and (26), if initially there are no SGWs ($C_{1,2} = 0$), the generated SFH amplitudes ($Q_{1,2}$) are:

$$Q_1(k_x, k_y) = \frac{1}{2\Omega_0} \left| \int_{t_0}^{t_f} I(k_x, k_y, t') \exp(i\Omega_1 t') dt' \right|, \quad (28)$$

$$Q_2(k_x, k_y) = \frac{1}{2\Omega_0} \left| \int_{t_0}^{t_f} I(k_x, k_y, t') \exp(i\Omega_2 t') dt' \right|. \quad (29)$$

One can replace the limits of integration by $\pm\infty$. After integration in time this

yields:

$$\begin{aligned}
Q_{1,2} &= \frac{\pi k_x}{\tilde{k}^3} \left(\frac{A}{2\Omega_0} \mp \frac{k_x}{\tilde{k}} \right) \exp \left[-\frac{(\Omega_0 \mp A/2)\tilde{k}}{Ak_x} \right] \\
&\quad \times \int \tilde{F}(k_x, k_y, k_z) \exp \left(-i \frac{(\Omega_0 \mp A/2)k_z}{Ak_x} \right) dk_z \\
&= \frac{2\pi^2 k_x}{\tilde{k}^3} \left(\frac{A}{2\Omega_0} \mp \frac{k_x}{\tilde{k}} \right) \exp \left[-\frac{(\Omega_0 \mp A/2)\tilde{k}}{Ak_x} \right] \\
&\quad \times F \left(k_x, k_y, -\frac{\Omega_0 \mp A/2}{Ak_x} \right), \tag{30}
\end{aligned}$$

Note that the last multipliers in Eq. (30) are proportional to the vorticity of initial perturbations at $z_{1,2} = -(\Omega_0 \mp A/2)/(Ak_x)$ respectively. The second multipliers indicates, that at small shear rates ($S \equiv A/\sqrt{4\tilde{k}g} \ll 1$), the amplitudes of generated SGWs are exponentially small with respect to the large parameter $1/S$. Equation (30) also indicates that for a fixed k_x , the generation has maximal effectiveness in two dimensional case ($k_y = 0$).

Let us describe the dynamic picture for a specific example, when pure internal vortex mode perturbation (without any admix of surface waves) is imposed in the flow initially. For simplicity we consider *two dimensional* problem, when $\partial/\partial y = 0$. The vertical velocity of the imposed perturbation is given by:

$$\begin{aligned}
u_z(x, z, t_0) &= z^3 \eta(-z) \exp \left(-\frac{[(z + z_0) \cos \phi + x \sin \phi]^2}{L_1^2} \right) \\
&\quad \times \exp \left(-\frac{[(z + z_0) \sin \phi - x \cos \phi]^2}{L_2^2} \right), \tag{31}
\end{aligned}$$

where $\eta(z)$ is Heaviside function, $(0, -z_0)$ is the center of the localization, $L_{1,2}$ characterize vertical and horizontal scales respectively and ϕ is the slope of the perturbation.

Numerical solution of the problem was performed as follows: Fourier transform of Eq. (31) with respect to x variable allows to determine $F(k_x, z)$ through Eq. (14). Another Fourier transform with respect to z yields $\tilde{F}(k_x, k_z)$. Then, the source function $I(k_x, t)$ is found by Eq. (20). Thus, the solution of the problem for a fixed k_x reduces to the numerical solution of the inhomogeneous equation, Eq. (19), with known $I(k_x, t)$.

Dependence of the source function $I(k_x, t)$ on t at $L_1 = 1$, $L_2 = 7$, $\phi = \pi/18$, $k_x = 1$, $z_0 = 2$ for two different values of the shear rate $S = 0.08$ (dashed line) and

$S = 0.32$ (solid line) is presented in Fig. 2. As it was mentioned above, the source term is localized function and considerably differs from zero only in the interval $t \in (20, 40)$ for $S = 0.08$ and $t \in (5, 10)$ for $S = 0.32$.

For analysis of the wave generation effectiveness it is useful to introduce the generation coefficients, that characterize the ratio of generated wave energy density and the maximum energy density of the initial vortex mode perturbations for a fixed value of k_x . Taking into account that the maximum energy density of the vortex mode perturbations is:

$$E_v = \frac{1}{2k_x^4} \int_{-\infty}^{\infty} |F(k_x, z)|^2 dz, \quad (32)$$

and the energy density of the generated waves:

$$E_{w1,2} = \frac{1}{k_x} Q_{1,2}^2(k_x), \quad (33)$$

we define the non-dimensional generation coefficients as:

$$G_{1,2} = Q_{1,2}(k_x) \left(\frac{2k_x^3}{\int_{-\infty}^{\infty} |F(k_x, z)|^2 dz} \right)^{1/2}. \quad (34)$$

Figure 3 represents generation coefficients G_1 (dashed line) and G_2 (solid line) vs shear rate S at $L_1 = 1$, $L_2 = 7$, $\phi = \pi/18$, $k_x = 1$ and $z_0 = 2$. As it can be seen, at small values of the shear rate, generation of SGW with frequency Ω_1 (i.e., propagating along x axis) considerably exceeds the generation of SGW with frequency Ω_2 (i.e., propagating against x axis), whereas the later wave is generated more effectively at $S > 0.15$.

The wave generation is well traced in Figs. 4 and 5, where the temporal evolution of the vertical component of velocity perturbation at the surface obtained by numerical solution of Eqs. (19)-(20) is presented for $S = 0.32$ and $S = 0.08$ respectively. The other parameters are the same as in Fig. 2. Purely internal vortex mode perturbation is imposed in the equations initially. The generation takes place in the time interval where $I(k_z, t)$ noticeably differs from zero. Afterward, just (two) waves with different frequencies and amplitudes exist. At $S = 0.32$, presented in Fig. 4, the generation takes place in the time interval $t \in (5, 10)$. Besides, SGW propagating against x axis is mainly generated. In contrast to this, at $S = 0.08$, presented in Fig. 5, the generation of SGW propagating along x axis is dominated. These numerical results are in agreement to analytical ones [see Eq. (30) and Fig. 3].

IV. DISCUSSION

In the previous sections simplified model was considered that allowed us to simplify mathematical description and study shear induced effects in the 'pure' form. For instance, the influence of the viscosity was ignored and the density ratio ρ_a/ρ_0 of the fluids above and below of the surface $z = 0$ was assumed to be zero. The later assumption allows to ignore all the dynamical processes in the upper fluid. On the other hand, it is well known that in the case of ocean waves the wind is the most important and powerful source of the waves. In this section we discuss possible applications of the studied linear effects to the concrete physical applications.

A. Ocean waves

It is well known [2, 3, 4, 5, 6] that the wind is main source of ocean SGWs. In the context of future discussion the papers of Chalikov group [23, 24] should also be noted, where the influence of small scale turbulence in the air on wave growth was studied in detail. At present there exists well developed theory both SGW generation and nonlinear evolution that is mainly confirmed by experiments as well as numerical simulations (for recent review see, e.g., [19]). After development of wind driven instability nonlinear 4-wave resonant interactions transfer the wave energy to smaller scales. Existing theory predicts that for relatively small frequencies Zakharov-Philonenko [20] spectrum $E(\omega) \sim \omega^{-4}$ of SGW fluctuations (sometimes called Toba's spectrum) should be observed (in this context see also [21]), whereas for relatively high wave numbers nonlinearity becomes strong and Phillips's spectrum $E(\omega) \sim \omega^{-5}$ of the wave turbulence should develop. Existing observations confirm this predictions and provide that in the range $\omega_p/3 < \omega < 3\omega_p$, where ω_p is the peak frequency, Zakharov-Philonenko spectrum is usually observed. For $\omega > 3\omega_p$ the spectrum becomes very close to Phillips's one [19]. The properties of the wave spectrum in the very short wavelength region, as well as dynamics of SGW turbulent fluctuations dissipation is much more unclear [22].

In the case of ocean waves presented linear mechanism of SGW generation can have important contribution to the balance of small scale SGW fluctuations. Indeed,

characteristic length scale of the turbulence at the ocean surface is much smaller than in the air. Namely, the characteristic length and velocity scales are $u_* \sim 1 \text{ cm/sec}$ and $l \sim 1 \text{ cm}$ respectively [25]. On the other hand, in the presence of the wind strong velocity shear $A \sim 10 \text{ sec}^{-1}$ is presented in so called 'buffer layer' [26] of the water, with the thickness $l_1 \sim (20 - 100)l_0$, where $l_0 \approx \nu/u_*$ is the dissipation length scale and ν is kinematic viscosity of the water. Simple estimates yields $l_1 \sim (0.5 - 1) \text{ cm}$. Presented linear mechanism implies that vortical perturbations generate SGWs with the same length scale. Therefore in the case of ocean waves internal vortex mode perturbations should effectively generate small scale SGWs - with the wavelength just above the capillary length scale $\lambda_c = 0.39 \text{ cm}$ [27]. In this context the study of the influence of capillary effects on the processes discussed above seems to be interesting. Analysis of this problem will be presented elsewhere.

B. Interfacial gravity waves

In the analysis presented in Secs. II and III density ratio ρ_a/ρ_0 of the fluids above and below of the surface $z = 0$ was assumed to be zero. Obtained results can be readily generalized in the case of interfacial GWs. If the density of upper and lower fluids are ρ_1 and ρ_2 and the shear rates are A_1 and A_2 respectively, then shear modified dispersion of interfacial GWs is given by the same expression (22) with g and A replaced by g_* and A_* , where

$$g_* = g \frac{\rho_2 - \rho_1}{\rho_2 + \rho_1}, \quad A_* = \frac{A_2 \rho_2 - A_1 \rho_1}{\rho_2 + \rho_1}. \quad (35)$$

From this equation it follows, that the influence of shear both on the wave dispersion and coupling with internal vortex perturbations, that is determined by dimensionless parameter

$$S_* \equiv \frac{A_*}{\sqrt{4\tilde{k}g_*}} = S_2 \frac{1 - \rho_1 A_1 / \rho_2 A_2}{\sqrt{1 - \rho_1^2 / \rho_2^2}} \quad (36)$$

is much more notable when the fluids have comparable densities if $\rho_1 A_1$ is not very close to $\rho_2 A_2$. Therefore, described shear induced effects usually should have much more influence on the dynamics of interfacial waves, then on the ocean waves.

V. SUMMARY

Let us summarize the main features of the linear dynamics of surface gravity waves in a simplified deep fluid (at $z < 0$) flow with vertical shear of the mean velocity $\mathbf{U}_0 = (Az, 0, 0)$. The simplification lies in the neglecting of the fluid compressibility and stratification, in other words, in the consideration of the system containing just two modes of perturbation: surface gravity wave mode and internal vortex mode. Special features of SGW in the system are the following:

The mean flow velocity shear causes the non-trivial modification of the frequencies and phase velocities of SGWs. The frequencies are defined by Eq. (22). The phase velocity becomes anisotropic [see Eq. (23) and Fig. 1]: its value is minimal for SFH propagating along x axis [$V_{ph}^{\min} = \sqrt{g/\tilde{k}(\sqrt{1+S^2} - S)}$] and maximal for SFH propagating against x axis [$V_{ph}^{\min} = \sqrt{g/\tilde{k}(\sqrt{1+S^2} + S)}$].

The mean flow velocity shear leads to the appearance of the intrinsic (to the fluid) source of SGW generation via coupling the wave with the internal vortex mode perturbations - the coupling results the emergency/generation of SGWs by internal vortex mode perturbations at $S \gtrsim 0.05$. The generation is different for the waves propagating in the different directions [see Eq. 30]. Generation of SGW with frequency Ω_1 considerably exceeds the generation of SGW with frequency Ω_2 for relatively small shear rates S , whereas the later wave is generated more effectively for the high shear rates ($S > 0.15$).

Acknowledgments

This research is supported by ISTC grant G 553.

The work was supported in part by the Department of Energy Grant No. DE-FG03-96ER-54346.

-
- [1] W. Kelvin, *Phylos. Mag.* **42**, 368 (1871).
 - [2] P. O. Phillips, *J. Fluid. Mech.* **2**, 417 (1957).
 - [3] J. W. Miles, *J. Fluid. Mech.* **3**, 185 (1957).

- [4] J. W. Miles, *J. Fluid. Mech.* **6**, 585 (1959).
- [5] J. W. Miles, *J. Fluid. Mech.* **10**, 496 (1961).
- [6] J. W. Miles, *J. Fluid. Mech.* **13**, 433 (1962).
- [7] K. Kajiura, *J. Oceanogr. Soc. Japan.* **18**, 51 (1962).
- [8] K. Kajiura, *J. Oceanogr. Soc. Japan.* **28**, 32 (1972).
- [9] H. C. Kranzer and J.B. Keller, *J. Appl. Phys.* **30**, 398 (1959).
- [10] P. Goldreich and D. Lynden-Bell, *Mon. Not. R. Astron. Soc.* **130**, 125 (1965).
- [11] W. O. Criminale and P. G. Drazin, *Stud. Appl. Math.* **83**, 123 (1990).
- [12] G. D. Chagelishvili, A. D. Rogava and D. G. Tsiklauri, *Phys. Rev. E* **53**, 6028 (1996).
- [13] S. J. Chapman, *J. Fluid Mech.* **451**, 35 (2002).
- [14] G. D. Chagelishvili, A. G. Tevzadze, G. Bodo, and S. S. Moiseev, *Phys. Rev. Lett.* **79**, 3178 (1997).
- [15] G. D. Chagelishvili, R. G. Chanishvili, J. G. Lominadze and A. G. Tevzadze, *Phys. Plasmas* **4**, 259 (1997).
- [16] A. D. Rogava, S. Poedts, and S.M. Mahajan, *Astron. Astrophys.* **354**, 749 (2000).
- [17] A. D. D. Craik, *J. Fluid Mech.* **37**, 531 (1968).
- [18] V. I. Shrira, *J. Fluid Mech.* **252**, 565 (1993).
- [19] P. Janssen, *The Interaction of Ocean Waves and Wind* (Cambridge Univ. Press, 2004).
- [20] V. E. Zakharov and N. N. Philonenko, *Sov. Phys. Doklady* **11**, 881 (1967).
- [21] S.A. Kitaigorodskii, *J. Phys. Oceanogr.* **13**, 816 (1983).
- [22] V. E. Zakharov, *Eur. J. Mech. B* **18**, 327 (1999).
- [23] D. V. Chalikov, *Sov. Phys. Doklady* **229**, 1083 (1976).
- [24] D. V. Chalikov and V. K. Makin, *Boundary layer Meteorol.* **56**, 83 (1991).
- [25] S.A. Kitaigorodskii and J. L. Lumley, *J. Phys. Oceanogr.* **13**, 1977 (1983).
- [26] P. A. Chang, U. Piomelli and W. K. Blake, *Phys. Fluids* **11**, 3434 (1999).
- [27] L.D. Landau and E.M. Lifshits, *Hydrodynamics* (Nauka, Moscow, 1988), p. 336.

FIG. 1: Shear induced anisotropy of SGW propagation: The leading wave crest at three different moments of time t_1 , t_2 , t_3 , when $t_2 = 2t_1$, $t_3 = 3t_1$, that are circular, but not concentric. A point source of the SGW is located at $x = y = 0$.

FIG. 2: $I(k_x, k_y, t)$ vs time at $S = 0.32$ (solid line) and $S = 0.08$ (dashed line) $k_x = 1$, $L_1 = 1$, $L_2 = 7$, $z_0 = 2$ and $\phi = \pi/18$.

FIG. 3: Generation coefficients G_1 (dashed line) and G_2 (solid line) vs. shear rate S at $k_x = 1$, $L_1 = 1$, $L_2 = 7$, $z_0 = 2$ and $\phi = \pi/18$.

FIG. 4: $u_z(k_x, t)$ vs. time at $S = 0.32$, $k_x = 1$, $L_1 = 1$, $L_2 = 7$, $z_0 = 2$ and $\phi = \pi/18$.

FIG. 5: $u_z(k_x, t)$ vs. time at $S = 0.08$, $k_x = 1$, $L_1 = 1$, $L_2 = 7$, $z_0 = 2$ and $\phi = \pi/18$.

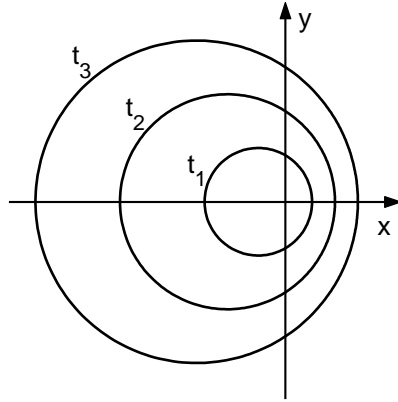


FIG. 1:

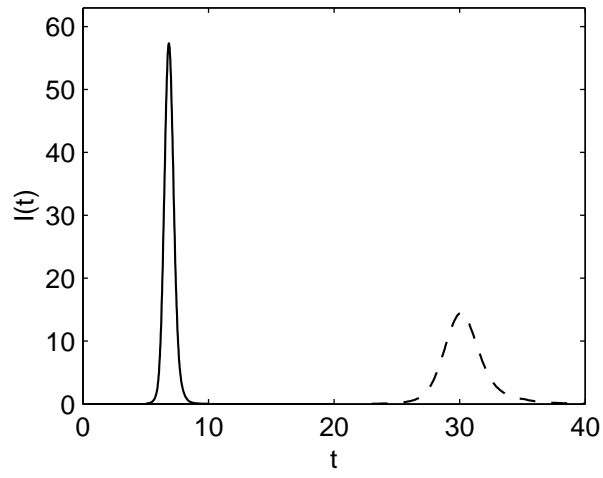


FIG. 2:

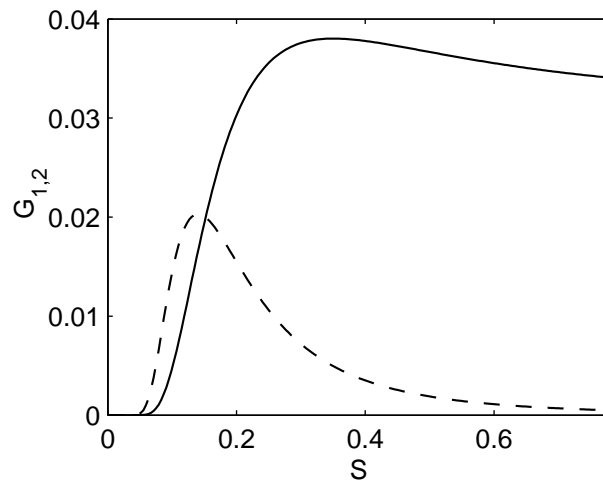


FIG. 3:

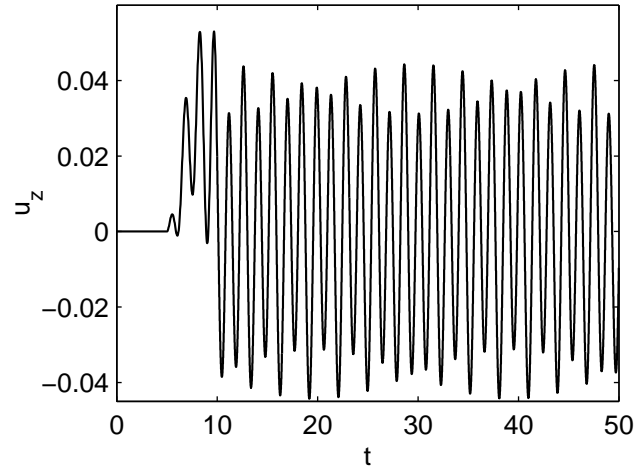


FIG. 4:

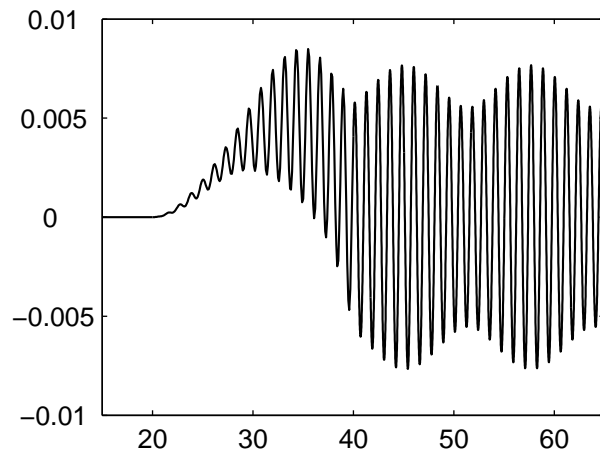


FIG. 5: